2-D08 mediates notable anticancer effects through multiple cellular pathways in uterine leiomyosarcoma cells

HOSOUK JOUNG[1] and HYUNJU LIU[2,3]

[1]Research Institute of Medical Sciences, Chonnam National University Medical School, Hwasun, Jeonnam 58128, Republic of Korea; [2]Department of Obstetrics and Gynecology, Chosun University College of Medicine, Gwangju 61452, Republic of Korea; [3]Department of Obstetrics and Gynecology, Chosun University Hospital, Gwangju 61453, Republic of Korea

Received February 2, 2024; Accepted May 29, 2024

DOI: 10.3892/or.2024.8756

Abstract. 2',3',4'-trihydroxyflavone (2-D08), a SUMO E2 inhibitor, has several biological functions, including anticancer activity, but its effects on uterine leiomyosarcoma (Ut-LMS) are unknown. The anticancer activity of 2-D08 was explored in an *in vitro* model using SK-LMS-1 and SK-UT-1B cells (human Ut-LMS cells). Treatment with 2-D08 inhibited cell viability in a dose- and time-dependent manner and significantly inhibited the colony-forming ability of Ut-LMS cells. In SK-UT-1B cells treated with 2-D08, flow cytometric analysis revealed a slight increase in apoptotic rates, while cell cycle progression remained unaffected. Western blotting revealed elevated levels of RIP1, indicating induction of necrosis, but LC3B levels remained unchanged, suggesting no effect on autophagy. A lactate dehydrogenase (LDH) assay confirmed increased LDH release, further supporting the induction of apoptosis and necrosis by 2-D08 in SK-UT-1B cells. 2-D08-induced production of reactive oxygen species and apoptosis progression were observed in SK-LMS-1 cells. Using Ki67 staining and bromodeoxyuridine assays, it was found that 2-D08 suppressed proliferation in SK-LMS-1 cells, while treatment for 48 h led to cell-cycle arrest. 2-D08 upregulated p21 protein expression in SK-LMS-1 cells and promoted apoptosis through caspase-3. Evaluation of α-SM-actin, calponin 1 and TAGLN expression indicated that 2-D08 did not directly initiate smooth muscle phenotypic switching in SK-LMS-1 cells. Transcriptome analysis on 2-D08-treated SK-LMS-1 cells identified significant differences in gene expression and suggested that 2-D08 modulates cell-cycle- and apoptosis-related pathways. The analysis identified several differentially expressed genes and significant enrichment for biological processes related to DNA replication and molecular functions associated with the apoptotic process. It was concluded that 2-D08 exerts antitumor effects in Ut-LMS cells by modulating multiple signaling pathways and that 2-D08 may be a promising candidate for the treatment of human Ut-LMS. The present study expanded and developed knowledge regarding Ut-LMS management and indicated that 2-D08 represents a notable finding in the exploration of fresh treatment options for such cancerous tumors.

Correspondence to: Professor Hyunju Liu, Department of Obstetrics and Gynecology, Chosun University College of Medicine, 309 Pilmun-daero, Dong-gu, Gwangju 61452, Republic of Korea
E-mail: lhj@chosun.ac.kr

Abbreviations: 2-D08, 2',3',4'-trihydroxyflavone; BrdU, bromodeoxyuridine; CHX, cycloheximide; DEGs, differentially expressed genes; FC, fold change; GO, gene ontology; LDH, lactate dehydrogenase; NAC, N-acetyl-L-cysteine; RASD1, dexamethasone-induced Ras-related protein 1; RNA-seq, RNA-sequencing; ROS, reactive oxygen species; SEM, standard error of the mean; SM, smooth muscle; Ut-LMS, uterine leiomyosarcoma; Ut-SMCs, uterine smooth muscle cells

Key words: 2-D08, uterine, leiomyosarcoma, SK-LMS-1, SK-UT-1B, apoptosis, proliferation

Introduction

Uterine leiomyosarcoma (Ut-LMS) is a malignant tumor of the smooth muscles of the uterus (myometrium). It is an uncommon disease that accounts for <1% of uterine malignancies and 25-36% of uterine sarcomas (1,2), but can spread to the surrounding tissues and organs (3). The 5-year disease-specific survival rate for patients with stage 3 or 4 Ut-LMS is 29-45% (4). Disease symptoms include abdominal pain and vaginal bleeding. A surgical biopsy should be performed to differentiate between Ut-leiomyoma and Ut-LMS because of the largely indistinguishable tissue appearance (5). Although Ut-leiomyomas rarely progress to Ut-LMS, Ut-leiomyomas may be a precursor form of Ut-LMS. If the tumor grows quickly or Ut-LMS is suspected after an ultrasound scan, it is necessary to periodically monitor whether it progresses to a malignant tumor, and additional examinations, such as MRI, are required.

Early diagnosis of Ut-LMS, based on a few methods before curative surgery, is difficult and studies on new biomarkers and the molecular mechanisms of Ut-LMS that could help overcome these challenges are scarce. For instance, activation of the Akt-mTOR pathway plays a key role in Ut-LMS development (6), and inhibitors of the PI3K and mTOR pathways suppress Ut-LMS growth both *in vitro* and *in vivo* (7). In addition, PTK787, a VEGFR/PDGFR inhibitor, can influence Ut-LMS tumor survival (8). LMP2 deficiency in mice leads

to spontaneous development of Ut-LMS, and aberrant expression of LMP2 may be a strong risk factor for Ut-LMS (9). A previous study on Ut-LMS involving The Cancer Genome Atlas network identified mutations and deletions corresponding to cancer genes such as *RB1*, tumor protein p53 and *PTEN* (10). In addition, other similar studies using whole-exome sequencing of Ut-LMS demonstrated frequent mutations in the *tumor protein p53*, *RB1, ATRX* and *MED12* genes (11,12).

Sustained cellular proliferation is a key hallmark of malignant tumors, and leiomyosarcomas are characterized by notable levels of proliferative activity (13). Several studies have been published regarding leiomyosarcoma and the presence of Ki67, which is a marker of cell proliferation. Ki67 is recognized as a predictive and prognostic indicator of various cancers, including breast (14,15), prostate (16,17) and adrenocortical carcinoma (18). A number of studies proposed that Ki67 holds prognostic significance in leiomyosarcoma as well (19,20).

2',3',4'-trihydroxyflavone (2-D08) is a synthetic flavone that mechanistically has been identified as a specific inhibitor of protein SUMOylation (21). Previous studies have demonstrated that 2-D08 has various biological functions, including anticancer activity. For example, 2-D08 has novel antiaggregatory and neuroprotective effects against amyloid-beta protein neurotoxicity in Alzheimer's disease (22) and inhibits the migration of pancreatic cancer cells by inducing K-Ras deSUMOylation (23). In addition, 2-D08 promotes apoptosis by inducing the accumulation of reactive oxygen species (ROS) in acute myeloid leukemia cells, probably via NOX2 deSUMOylation (24). Lastly, 2-D08 treatment negatively influences C2C12 myoblast cell proliferation and differentiation (25).

The effect of 2-D08 on the growth of Ut-LMS is not fully understood. In the present study, the anticancer effects induced by 2-D08 in human LMS cell lines were explored and the potential underlying molecular mechanisms were investigated.

Materials and methods

Cell lines and reagents. The human Ut-LMS cancer cell lines SK-LMS-1 (cat. no. HTB-88) and SK-UT-1B (cat. no. HTB-115) were purchased from the American Type Culture Collection. The cells were cultured in a humidified incubator maintained in Minimum Essential Medium (cat. no. LM007-07; Welgene, Inc.) containing 10% fetal bovine serum (cat. no. SH30919.03; Hyclone; Cytiva) and 1% streptomycin-penicillin (cat. no. 15140122; Gibco; Thermo Fisher Scientific, Inc.) at 37˚C with 5% CO_2. The human uterine smooth muscle cells (Ut-SMCs; cat. no. C-12575) were purchased from PromoCell GmbH and were cultured in smooth muscle cell growth medium 2 (cat. no. C-39267; PromoCell GmbH) supplemented with 1% streptomycin-penicillin. 2-D08 was obtained from MilliporeSigma (cat. no. SML1052-5MG). Dimethyl sulfoxide (cat. no. DMS555.500; BioShop Canada Inc.) was used as a control. Cycloheximide (CHX) solution (cat. no. C4859-1ML), N-acetyl-L-cysteine (NAC; cat. no. A7250), and catalase (CAT; cat. no. C1345) were purchased from Sigma-Aldrich; Merck KGaA.

MTT assays. The cells ($5x10^3$ cells per well) were seeded in 96-well plates for 24 h and then treated with different concentrations of 2-D08 for 24 or 48 h. MTT stock solution (cat. no. M2128; Sigma-Aldrich) was added to each well, before incubation at 37˚C for 2 h 30 min and addition of dimethyl sulfoxide (150 μl per well) to all wells after removing the medium. Cell viability was measured at 570 nm using an INNO microplate spectrophotometer (LTEK Co., Ltd.) and normalized to that of the control group.

Colony formation assay. SK-LMS-1 and SK-UT-1B cells were seeded in 6-well plates ($1x10^3$ cells per well) for 24 h. After removing the medium, 2-D08 was added to a fresh medium containing different concentrations (10, 20, 50, and 100 μM). The cells were cultured at 37˚C for 7 days until colonies were visible. To observe colony growth, a crystal violet assay kit (cat. no. ab232855; Abcam) was employed following the manufacturer's protocol. In brief, the cells were fixed with 100% ice-cold methanol for 20 min at -20˚C, stained with 2% crystal violet solution for 20 min at room temperature, and colonies containing ≥50 cells were counted. Bright-field microscopy images of the formed colonies were acquired using the EVOS FL Cell Imaging System (Thermo Fisher Scientific, Inc.). The surviving fraction was calculated as the mean number of colonies/[number of inoculated cells x (plating efficiency/100)]. Plating efficiency was defined as 100x (mean number of colonies/number of inoculated cells for control). Survival curves were determined using a linear-quadratic model with the GraphPad Prism 6.0 software (GraphPad; Dotmatics).

Lactate dehydrogenase (LDH) assay. LDH was quantified using the Dyne LDH PLUS Cytotoxicity Assay Kit (cat. no. GBL-P500; Dyne Bio Inc.) according to the manufacturer's instructions. Briefly, the cells were treated with 2-D08 at 37˚C for 24 or 48 h, as indicated. Subsequently, 100 μl of supernatant was transferred from each well to a new 96-well plate, followed by the addition of 100 μl of LDH PLUS Reaction Mixture to each well and a gentle mix. The plates were incubated at room temperature, protected from light, for 30 min before adding 10 μl of stop solution to each well and being gently mixed. The LDH concentration was measured at 490 nm and the treated groups were compared with the untreated.

ROS quantification using flow cytometry. Flow cytometric measurement of ROS production was performed using a Muse Oxidative Stress Kit (cat. no. MCH100111; Luminex) according to the manufacturer's instructions. Briefly, SK-LMS-1 cells were seeded in 6-well plates ($5x10^4$ cells/well) and allowed to grow at 37˚C for 24 h. The cells were then pretreated with 0, 20, 50, or 100 μM 2-D08, diluted in fresh medium at 37˚C, for 24 and 48 h. Next, the cells were detached and resuspended in 1X Assay Buffer, and Muse Oxidative Stress Reagent working solution was added. The samples were incubated for 30 min at 37˚C before analysis using the Guava Muse Cell Analyzer (cat. no. 0500-3115; Luminex), and further analyzed using Muse analysis software (version 1.5; Luminex).

Flow cytometric analysis of apoptosis. The apoptotic profiles were studied using the Muse Annexin V & Dead Cell Kit (cat. no. MCH100105; Luminex). Annexin V-PE detects phosphatidylserine on the external membrane of apoptotic cells,

while 7-AAD permeates late-stage apoptotic and dead cells by being excluded from live and healthy cells. Ut-LMS cells were treated with 2-D08 at different concentrations (20, 50, or 100 μM) for 24 or 48 h in 6-well plates at $5x10^4$ cells per well. The cells were trypsinized, harvested, and resuspended in a fresh medium. Then, 100 μl of Muse Annexin V & Dead Cell reagent was added. After staining for 20 min at room temperature in the dark, the apoptotic profiles of the cells were recorded using the Guava Muse Cell Analyzer following the manufacturer's instructions and further analyzed using Muse analysis software (version 1.5; Luminex).

Ki67 immunostaining. SK-LMS-1 cells were fixed with IC Fixation Buffer (cat. no. 00-8222-49; Invitrogen; Thermo Fisher Scientific, Inc.) for 20 min at room temperature and permeabilized with 0.2% Triton X-100 (cat. no. T8787-50ML; Sigma-Aldrich) in 1X phosphate-buffered saline (cat. no. LB 001-02; Welgene, Inc.) for 5 min at room temperature. The cells were then blocked with 2% normal goat serum (cat. no. 5425; Cell Signaling Technology, Inc.) in phosphate-buffered saline and incubated with the anti-Ki67 antibody (1:250; cat. no. MA5-14520; Invitrogen; Thermo Fisher Scientific, Inc.) at 4˚C overnight. The anti-Ki67 antibody was detected by incubating the cells with an anti-rabbit IgG antibody (Fab2 Alexa Fluor 594 Conjugate; 1:500; cat. no. 8889S; Cell Signaling Technology, Inc.) for 1 h at room temperature. The slides were mounted using ProLong Gold Antifade Mountant with DAPI (cat. no. P36935; Invitrogen; Thermo Fisher Scientific, Inc.). Fluorescence images were obtained using the EVOS FL Cell Imaging System.

Flow cytometric assessment of Ki67 expression. To determine the percentage of proliferating cells based on Ki67 expression, the Muse Ki67 Proliferation Kit (cat. no. MCH10014; Luminex) was used. Briefly, cells expressing Ki67 were harvested, fixed with 1X fixation solution for 15 min at room temperature, and washed with 1X assay buffer. After resuspension, the cells were treated with permeabilization solution for 15 min at room temperature and washed again. Next, the cells were incubated with either Muse Hu IgG1-PE or Muse Hu Ki67-PE antibody for 30 min at room temperature and analyzed using the Guava Muse Cell Analyzer, followed by further analysis using Muse analysis software (version 1.5; Luminex).

Bromodeoxyuridine (BrdU) cell proliferation assay. The BrdU Cell Proliferation Assay Kit (cat. no. 6831S; Cell Signaling Technology, Inc.) was used to study the proliferating cells. In brief, cells ($5x10^3$ cells/well) were seeded into 96-well plates and treated with 2-D08 at the indicated concentrations for 24 or 48 h. The cells were then exposed to BrdU at 37 ˚C for 24 h, fixed at room temperature for 30 min, and incubated with mouse anti-BrdU antibody at room temperature for 1 h, and treated according to the manufacturer's protocol. Lastly, the absorbance was measured at 450 nm using an INNO microplate spectrophotometer.

Flow cytometric evaluation of cell cycle distribution. The Muse Cell Cycle Kit (cat. no. MCH100106; Luminex) was used to determine the cell cycle phases of the samples. The cells were centrifuged and fixed for 3 h in 70% ethanol at -20˚C. After fixation, the cells were stained with the Muse Cell Cycle Reagent and incubated in the dark at room temperature for 30 min. The samples were analyzed using the Guava Muse Cell Analyzer, followed by further analysis using Muse analysis software (version 1.5; Luminex).

Protein preparation and western blot analysis. Ut-LMS cells were exposed to various concentrations of 2-D08 (0, 20, or 50 μM) for 48 h. The cells were then lysed in NP-40 lysis buffer (cat. no. MBS355472; MyBiosource, Inc.) containing a protease inhibitor cocktail (cat. no. P8340; Sigma-Aldrich; Merck KGaA). The Pierce BCA Protein Assay kit (cat. no. 23225; Thermo Fisher Scientific, Inc) was used to measure the protein concentration of lysate. Equal amounts of protein (10-50 μg from cell lysate), denatured by heating, were subjected to 12-15% SDS-PAGE. After electrophoresis, the separated proteins were transferred from the gel to PVDF membranes (cat. no. IPVH00010; Merck KGaA), which were blocked with 5% skimmed milk (cat. no. 262100; BD Biosciences) for 1 h at room temperature, and subsequently incubated with the primary antibodies overnight at 4˚C with gentle shaking. The primary antibodies used in the present study were RIP (1:1,000; cat. no. 3493T), LC3B (1:1,000; cat. no. 2775S), p21 (1:1,000; cat. no. 2947S), p27 (1:1,000; cat. no. 3686T), p53 (1:1,000; cat. no. 2527S), Caspase-3 (1:1,000; cat. no. 9665S), cleaved Caspase-3 (1:1,000; cat. no. 9664S), Caspase-9 (1:1,000; cat. no. 9502S), PARP (1:1,000; cat. no. 9542S) and β-Actin (1:1,000; cat. no. 4967S) (all from Cell Signaling Technology, Inc.); and α-smooth muscle (SM) actin (1:1,000; cat. no. ab5694), TAGLN (1:5,000; cat. no. ab14106) and Calponin 1 (1:1,000; cat. no. ab46794) (all from Abcam). After washing with the TBST (Tris-buffered saline, 0.05% Tween 20) solution, the membranes were incubated with anti-rabbit (1:5,000; cat. no. 7074S; Cell Signaling Technology, Inc.) and anti-mouse horseradish peroxidase-conjugated secondary antibodies (1:5,000; cat. no. 7076S; Cell Signaling Technology, Inc.) for 1 h at room temperature. The signals were detected using the Immobilon ECL Ultra Western HRP Substrate (cat. no. WBKLS0100; Merck KGaA) and quantified using the Azure c280 chemiluminescent image system. Densitometric analyses of the resulting images were performed using ImageJ 1.53a software (National Institutes of Health).

Reverse transcription-quantitative PCR (RT-qPCR). Total RNA was extracted from SK-LMS-1 cells using NucleoZOL (cat. no. 740404.200; Macherey-Nagel GmbH & Co. KG). RNA samples were reverse transcribed into cDNA using a ReverTra Ace qPCR RT Kit (cat. no. FSQ-101; Toyobo Life Science). In brief, RNA was denatured at 65˚C for 5 min, then placed on ice. The reaction solution was prepared with nuclease-free water, 5X RT buffer, RT enzyme mix, primer mix, and RNA (0.5 pg-1 μg) to a total volume of 10 μl. The mixture was incubated at 37˚C for 15 min, heated at 98˚C for 5 min, and then stored at 4˚C or -20˚C. RT-qPCR was performed using a QuantiTect SYBR Green RT-PCR Kit (cat. no. 204243; Qiagen GmbH) and the primer pairs listed in Table SI. The cycling conditions included an initial denaturation step at 95˚C for 10 min. Amplification was carried out for 40 cycles with denaturation at 95˚C 15 sec, followed by annealing at 50˚C for 20 sec to achieve optimal annealing

temperatures, and extension at 72˚C for 20 sec. The RNA level was expressed as a relative result via the $2^{-\Delta\Delta Cq}$ method (26) against the endogenous standard control β-actin.

RNA-sequencing (RNA-seq). Total RNA was extracted from SK-LMS-1 cells using NucleoSpin RNA/Protein (cat. no. 740933.50; Macherey-Nagel GmbH & Co. KG) according to the manufacturer's instructions. RNA quality was assessed with a 4200 TapeStation System with an RNA Screen Tape (Agilent Technologies, Inc.), and RNA was quantified using a Qubit fluorometer (Thermo Fisher Scientific, Inc.). Libraries with total RNAs were constructed using the KAPA RNA HyperPrep Kit with RiboErase (cat. no. 08098140702; Roche Sequencing Solution, Inc.) according to the manufacturer's instructions. The loading concentration of the final library was measured using the TapeStation 4200 System (Agilent Technologies, Inc.) and qPCR was performed on the LightCycler 480 System (Roche Diagnostics) with the Kapa Library Quantification Kit (cat. no. 07960298001; Roche Sequencing Solution, Inc.), resulting in the final library being loaded at 2 nM. High-throughput sequencing was performed in paired-end 150 sequencing runs using a NovaSeq 6000 (Illumina, Inc.) at Genome Insight, Inc. Raw reads were assembled and low-quality reads were filtered using Cutadapt (v.3.4; National Bioinformatics Infrastructure Sweden). Filtered reads were aligned on a reference genome downloaded from Ensembl (GRCh38; Homo sapiens; https://www.ensembl.org) using STAR (v.2.7.8a) (27) and the gene-level expression for each sample was calculated using RSEM (v.1.3.1) (28). Differentially expressed genes were analyzed using a two-slided Wald test under each condition with the DESeq2 (version 1.26.0) (29) and edgeR (version 3.28.1) (30) packages.

Statistical analysis. The GraphPad Prism software (v.6.0; Graphpad; Dotmatics) was used for the statistical analyses. The results are expressed as the mean ± standard error of the mean (SEM), and the data were analyzed using one-way analysis of variance, followed by Tukey's post hoc test for comparison among multiple groups. $^{*}P<0.05$ was considered to indicate a statistically significant difference.

Results

2-D08 inhibits the viability of Ut-LMS cells. The cytotoxic effect of 2-D08 treatment (Fig. 1A) on Ut-LMS cells was first investigated using the well-established SK-LMS-1 and SK-UT-1B cell models. The viability of Ut-LMS cells was determined using MTT assays followed by treatment with 2-D08 at different concentrations (0-100 μM) for 24 or 48 h. As revealed in Fig. 1B, the viability of SK-LMS-1 cells significantly decreased to 21% in the 100-μM 2-D08-treated group at 24 h, although different doses did not lead to statistically significant changes (Fig. 1B, left graph). After 48 h of treatment, SK-LMS-1 cell viability decreased significantly to 80 and 17% at 50 and 100 μM 2-D08 concentrations, respectively (Fig. 1B, right graph). Treatment of SK-UT-1B cells with 2-D08 at concentrations >10 μM for 24 and 48 h significantly inhibited cell viability (Fig. 1C). By contrast, treatment of normal Ut-SMCs with 2-D08 for 24 and 48 h had a slight inhibitory effect on viability (Fig. 1D). These results indicated that the viability of Ut-LMS cells was significantly affected by 2-D08 treatment.

2-D08 inhibits colony formation of Ut-LMS cells. It was investigated whether 2-D08 affects the proliferation of Ut-LMS cells using a colony formation assay. As demonstrated in the crystal violet-stained (upper panels) and bright-field images (lower panels) in Fig. 1E, the size of a single colony in the 2-D08-treated groups (20, 50 and 100 μM) after 7 days was smaller than that in the control group. Compared with control cells, treatment of Ut-LMS cells with 2-D08 (10, 20, 50, and 100 μM) for 7 days induced a dose-dependent decline in survival fraction (Fig. 1F). Furthermore, plating efficiency was measured to assess the colony-forming ability of Ut-LMS cells compared with that of untreated cells. The mean plating efficiency of Ut-LMS cells decreased significantly (Fig. 1G). These findings indicated that 2-D08 plays a key role in inhibiting colony formation and is a potential drug for clinical applications in Ut-LMS cells.

2-D08-induced apoptotic and necrotic cell death is dependent on RIP1 in SK-UT-1B cells. To determine whether the aforementioned reductions in cell viability induced by 2-D08 in SK-UT-1B cells were associated with apoptotic cell death and cell cycle arrest, a flow cytometric analysis was performed. Apoptotic cells were identified using Annexin V. As revealed in Fig. 2A, the percentage of apoptotic cells slightly increased in 2-D08-treated SK-UT-1B cells compared with that in untreated cells. Additionally, SK-UT-1B cells were stained with propidium iodide, and the cell cycle profiles were evaluated using the Guava Muse Cell Analyzer. The results indicated that treatment with 2-D08 did not affect the progression of the cell cycle in SK-UT-1B cells (Fig. 2B). To investigate whether 2-D08 regulates necrosis or autophagy in SK-UT-1B cells, the expression of RIP (a necrosis marker) and LC3B (an autophagy marker) were analyzed. Cells were treated with 2-D08 at the indicated concentrations, and the expression of RIP1 and LC3B was assessed using western blot analysis. The level of RIP1 was significantly higher in 2-D08-treated cells than in untreated cells, while that of LC3B remained unchanged (Fig. 2C). Furthermore, 2-D08-treated SK-UT-1B cells were evaluated using LDH assays to confirm necrosis. As shown in Fig. 2D, 2-D08 significantly increased the levels of LDH release in SK-UT-1B cells. These results suggested that 2-D08 significantly induces apoptosis and necrosis in SK-UT-1B cells.

2-D08 triggers intracellular ROS level increment. Excessive accumulation of ROS in cells can lead to oxidative stress, resulting in damage to nucleic acids, lipids, proteins, membranes and mitochondria (31). To assess whether 2-D08 increases ROS levels in SK-LMS-1 cells, the cells were cultured with different concentrations of 2-D08 (0, 20, 50 and 100 μM) for 24 and 48 h, followed by analysis with the Guava Muse Cell Analyzer. ROS levels were at 33.0, 43.0, 50.5 and 77.6% in control and 2-D08 treated SK-LMS-1 cells at the indicated concentration for 24 h, respectively (Fig. 3A, upper panels). After 48 h of 2-D08 treatment, the respective results were 43.7, 61.3, 82.55 and 88.48% (Fig. 3A, bottom panels).

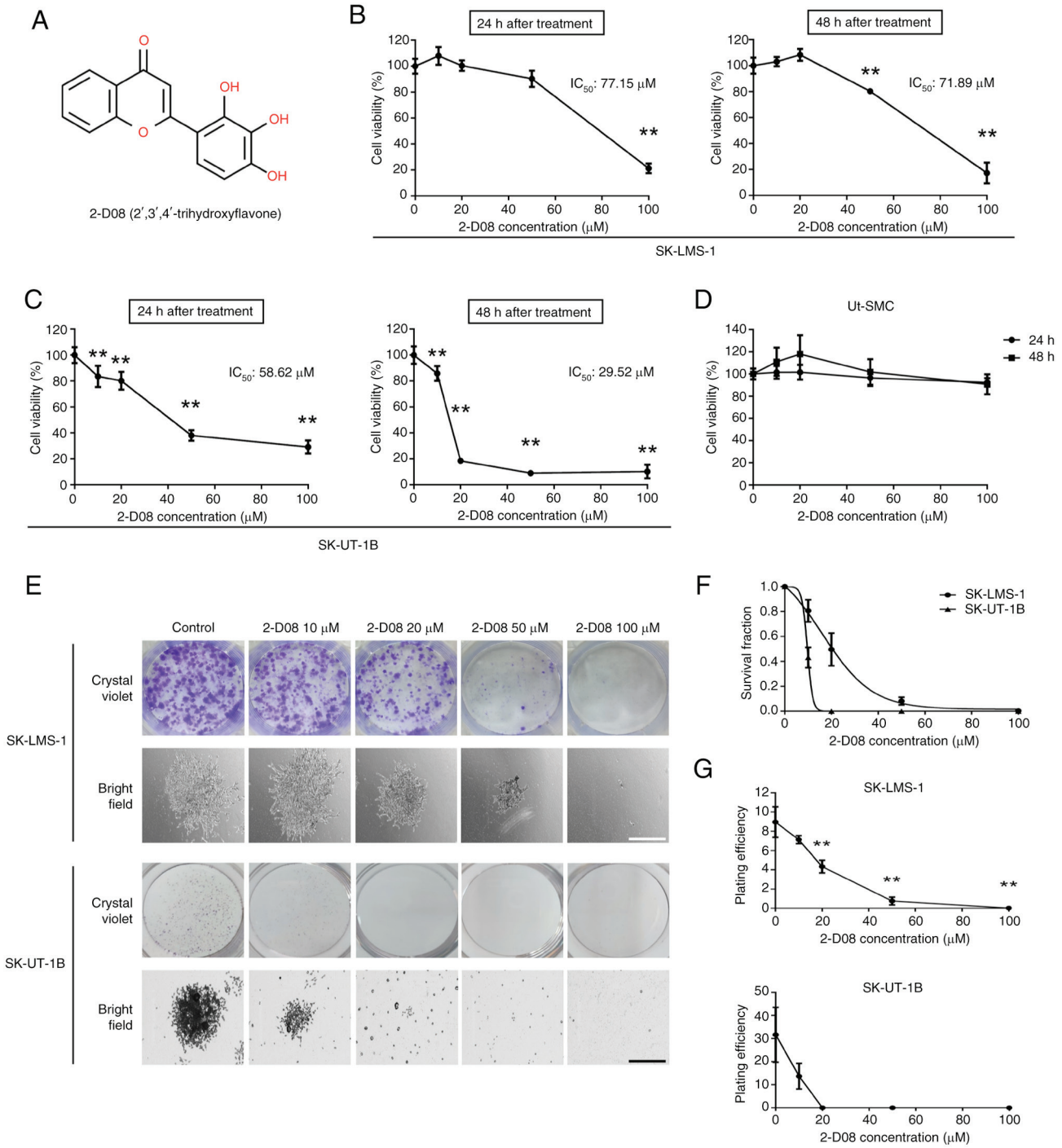

Figure 1. 2-D08 decreases viability and colony formation ability in the Ut-LMS cells. (A) Chemical structure of 2-D08. (B-D) Ut-LMS cells and Ut-SMCs were treated with various concentrations (0-100 μM) of 2-D08 for 24 or 48 h. After the end of incubation, cell viability was measured using MTT assays. Graphs of viability versus 2-D08 concentrations were used to calculate IC_{50} values based on the trendline equation for Ut-LMS cells. (E) Ut-LMS cells were treated with 2-D08 at the indicated concentration (0-100 μM) for 7 days. Representative microscopic images of the colonies stained using crystal violet (white scale bar, 1,000 μm; black scale bar, 400 μm). (F and G) After 7 days, dose-survival curves derived from a clonogenic survival assay and comparisons of plating efficiency were performed. Surviving fractions were calculated based on colony counts and plating efficiency. The data are reported as the mean ± SEM. All experiments were repeated thrice. **P<0.01 compared with the control group. 2-D08, 2',3',4'-trihydroxyflavone; Ut-LMS, uterine leiomyosarcoma; Ut-SMCs, uterine smooth muscle cells; SEM, standard error of the mean.

Consequently, these results indicated that 2-D08 induces ROS generation in SK-LMS-1 cells.

2-D08 promotes apoptosis in SK-LMS-1 cells. To examine whether cells undergo apoptosis, SK-LMS-1 cells were treated with different concentrations (20, 50, or 100 μM) of 2-D08 for 24 and 48 h. Apoptotic cells were determined in flow cytometry using Annexin V. As demonstrated in Fig. 3B, the percentage of apoptotic cells significantly increased in a dose-dependent manner. After 24 h of treatment, the percentages of apoptotic cells were 7.01% at 20 μM, 15.66% at 50 μM and 90.93% at 100 μM, compared with 5.56% for the control

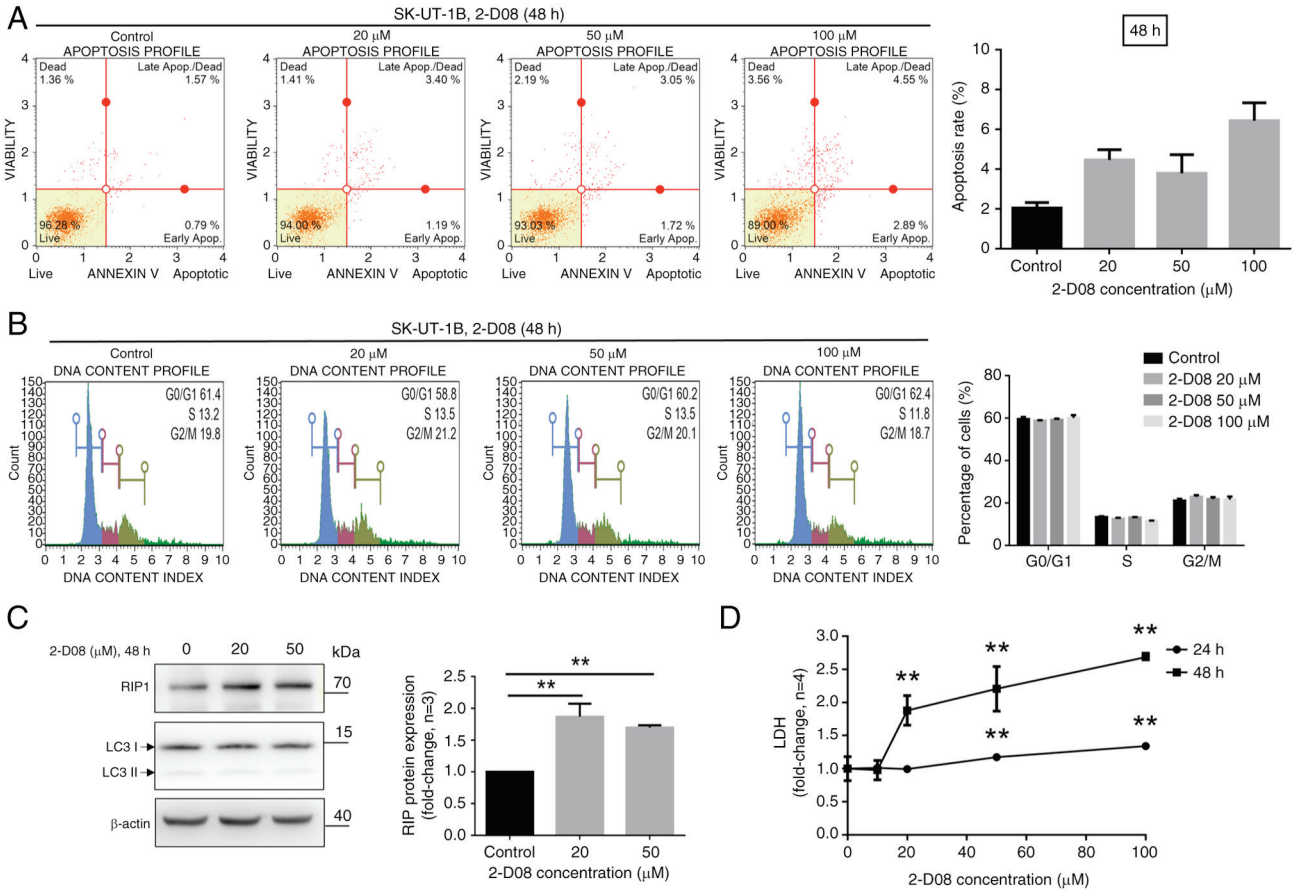

Figure 2. 2-D08-induced apoptotic and necrotic cell death is dependent on RIP1. (A and B) After treatment with 2-D08 at the indicated concentrations, SK-UT-1B cells were stained with Annexin V and propidium iodide to analyze the apoptotic rates and cell cycle distribution, respectively, using flow cytometry. The quantitative data are shown in the right panel. (C) Representative western blots of the necrosis marker RIP1 and autophagy maker LC3B. SK-UT-1B cells were treated with 2-D08 at 20 and 50 μM and the indicated proteins were analyzed 48 h after treatment. (D) *In vitro* LDH assay of SK-UT-1B cells. The cells were treated for 24 or 48 h with 2-D08 at indicated concentrations (10, 20, 50, or 100 μM) and the supernatants were analyzed for LDH content, as described in the materials and methods. Cell lysis solution served as a positive control for 100% cell lysis and LDH release. Three experiments were performed that showed similar results. The data are presented as the mean ± SEM. **P<0.01. 2-D08, 2',3',4'-trihydroxyflavone; LDH, lactate dehydrogenase; SEM, standard error of the mean.

cell culture (Fig. 3B, upper panels). After 48 h of treatment, the percentages of apoptotic cells were 8.81% at 20 μM, 16.77% at 50 μM, and 83.39% at 100 μM, compared with 6.53% for the control cell culture (Fig. 3B, bottom panels). To further identify whether ROS production is involved in 2-D08-induced apoptosis, SK-LMS-1 cells were treated with 2-D08 (100 μM) with or without NAC and CAT. Both NAC and CAT, known as ROS scavengers (32,33), effectively reduced 2-D08-induced apoptosis in SK-LMS-1 cells (Fig. 3C). These results indicated that 2-D08 induces ROS-mediated apoptosis in SK-LMS-1 cells. However, antioxidants, acting as ROS-scavengers, block the anticancer effect of 2-D08 on SK-LMS-1 cells.

2-D08 suppresses the proliferation of SK-LMS-1 cells in vitro. The aforementioned experiments demonstrated that a consistent proliferation inhibitory effect occurs with 20-50 μM 2-D08 and that high doses (100 μM) have the potential to induce non-specific cytotoxicity. Based on these findings, subsequent experiments were conducted using 20- and 50-μM doses at 48 h. Cell proliferation was assessed by evaluating Ki67 expression and using a BrdU assay. The expression of the proliferation marker Ki67 is demonstrated in Fig. 4A. To accurately quantify the expression of Ki67 in SK-LMS-1 cells, flow cytometry was utilized. The proportion of Ki67-positive cells decreased from 93.48 to 67.79 (20 μM) and 65.03% (50 μM) after a 48-h treatment with 2-D08 (Fig. 4B). BrdU incorporation in proliferating cells significantly decreased in 50-μM 2-D08-treated cells at 48 h compared with that in the control (n=10) (Fig. 4C). These results indicated that 2-D08 treatment induces antiproliferative effects in SK-LMS-1 cells.

2-D08-mediated S and G2/M arrest contributes to growth inhibition in SK-LMS-1 cells. To investigate whether 2-D08-mediated inhibition of cell proliferation is related to cell cycle arrest, SK-LMS-1 cells were treated with varying concentrations of 2-D08 for 24 and 48 h. The cell cycle profiles were assessed using the Guava Muse Cell Analyzer. Interestingly, 2-D08 significantly increased the cell population at the S and G2/M phases, while simultaneously reducing it in the G0/G1 phase after 48 h of treatment (Fig. 4D). This experiment confirmed that 2-D08-mediated cell cycle arrest contributes to inhibition of proliferation in SK-LMS-1 cells.

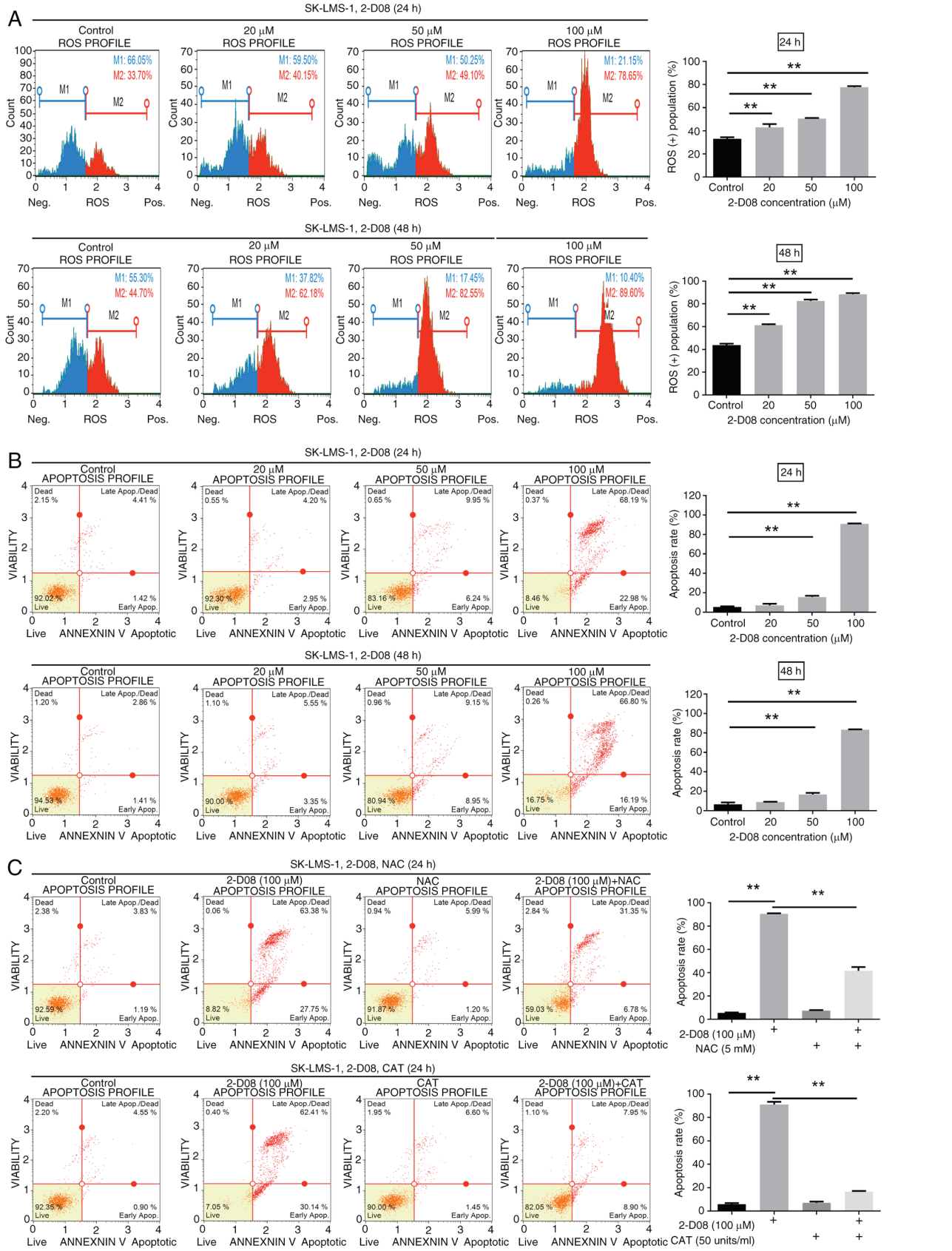

Figure 3. 2-D08 induces ROS production and apoptosis in SK-LMS-1 cells. (A) SK-LMS-1 cells were exposed to 2-D08 (0, 20, 50, or 100 μM) for 24 and 48 h. Intracellular ROS fluorescence signals were detected using the Muse Oxidative Stress kit, and typical ROS profile plots are shown. A similar pattern was observed in three independent experiments. The percentage of ROS-positive cells is revealed in the histogram graph (right). (B) SK-LMS-1 cells were treated with 0, 20, 50, or 100 μM of 2-D08 for 24 and 48 h. Apoptosis was decided using Annexin V staining and flow cytometry. Representative results are demonstrated in the left panel, and the statistical analysis is represented in the right panel. (C) Apoptosis was measured in SK-LMS-1 cells treated with 2-D08 (100 μM) in the presence or absence NAC (5 mM) and CAT (50 units/ml) for 24 h. NAC and CAT, acting as ROS scavengers, partly rescued the 2-D08-induced apoptosis in SK-LMS-1 cells. The data are expressed as the mean ± SEM; n=3. **P<0.01. 2-D08, 2',3',4'-trihydroxyflavone; ROS, reactive oxygen species; NAC, N-acetyl-L-cysteine; CAT, catalase; SEM, standard error of the mean.

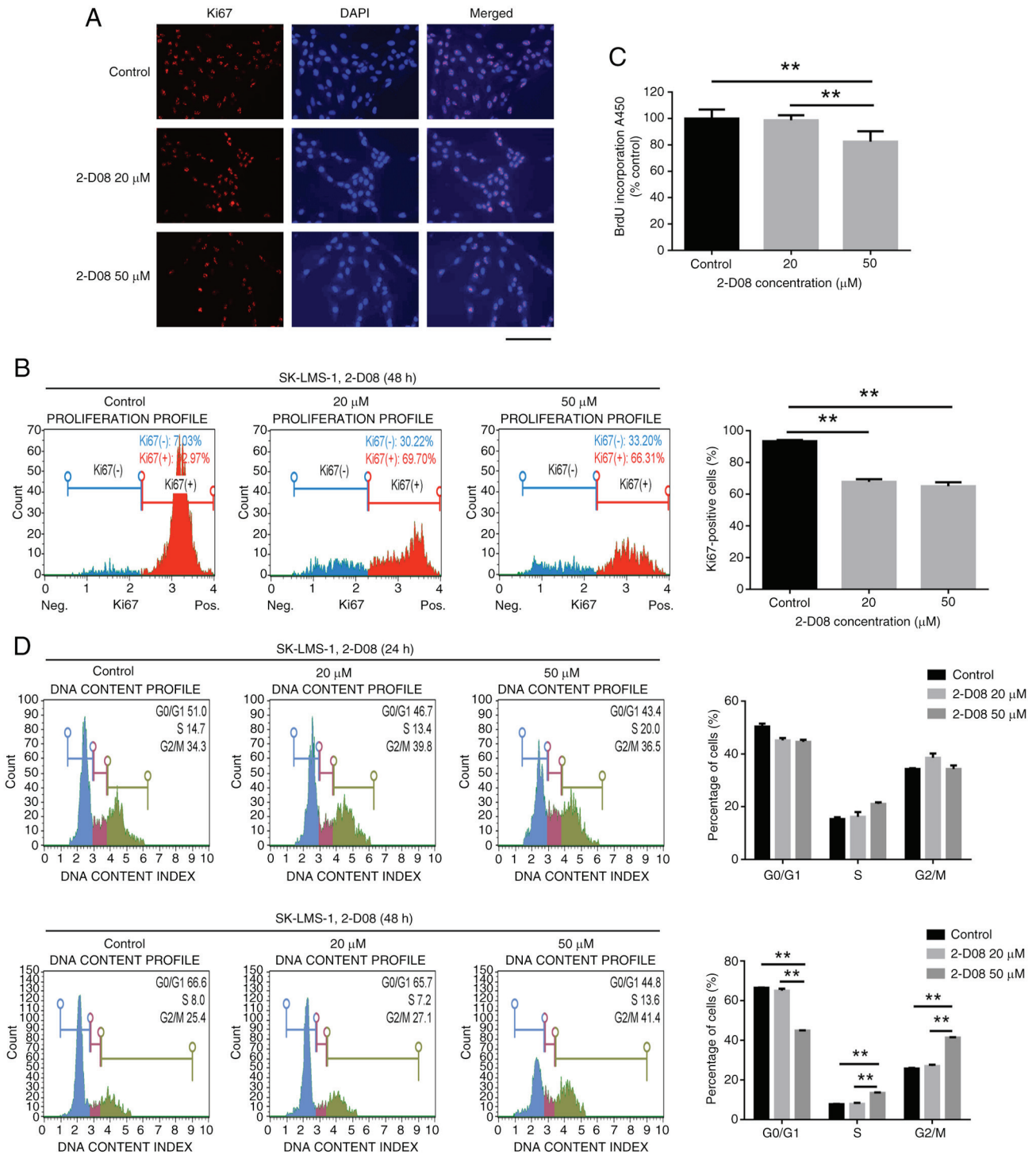

Figure 4. Inhibition of SK-LMS-1 cell proliferation and cell cycle by 2-D08. (A) SK-LMS-1 cells were treated with 20 and 50 μM of 2-D08 for 48 h, and immunofluorescence assays were used to analyze the expression of the cell proliferation marker Ki67 in the treated cells. Red, Ki67; blue, nuclear DNA. Scale bar, 200 μm. (B) The percentage of Ki67-positive cells at the indicated concentrations at 48 h. The Muse Ki67 Proliferation kit allowed for the quantification of the percentages of proliferating and non-proliferating cells based on Ki67 expression. (C) A BrdU assay was performed after 48 h of treatment of SK-LMS-1 cells with 2-D08 (20 or 50 μM). Absorbance was measured at 450 nm using a microplate reader. (D) SK-LMS-1 cells were treated with 2-D08 (0, 20, or 50 μM) for 24 and 48 h and then subjected to a DNA content analysis using flow cytometry. The left panel shows a representative histogram of the cell cycle distribution, while the right panel quantifies the cell cycle distributions. The data are presented as the mean ± SEM of three independent experiments. **P<0.01 compared with each group. 2-D08, 2',3',4'-trihydroxyflavone; SEM, standard error of the mean.

Effect of 2-D08 on the expression of proteins related to cell proliferation and apoptosis in SK-LMS-1 cells. To study the detailed mechanism(s) of action of 2-D08, western blotting was employed to detect the protein levels of the cell cycle-regulatory proteins p21, p27 and p53. Application of 2-D08 in the SK-LMS-1 cells significantly increased p21 protein levels at 20 and 50 μM, but not p53 levels. Treatment with the low dose of 2-D08 (20 μM) increased p27 levels, while, at a high dose (50 μM), no significant increase was observed (Fig. 5A). CHX assay was also conducted to inhibit

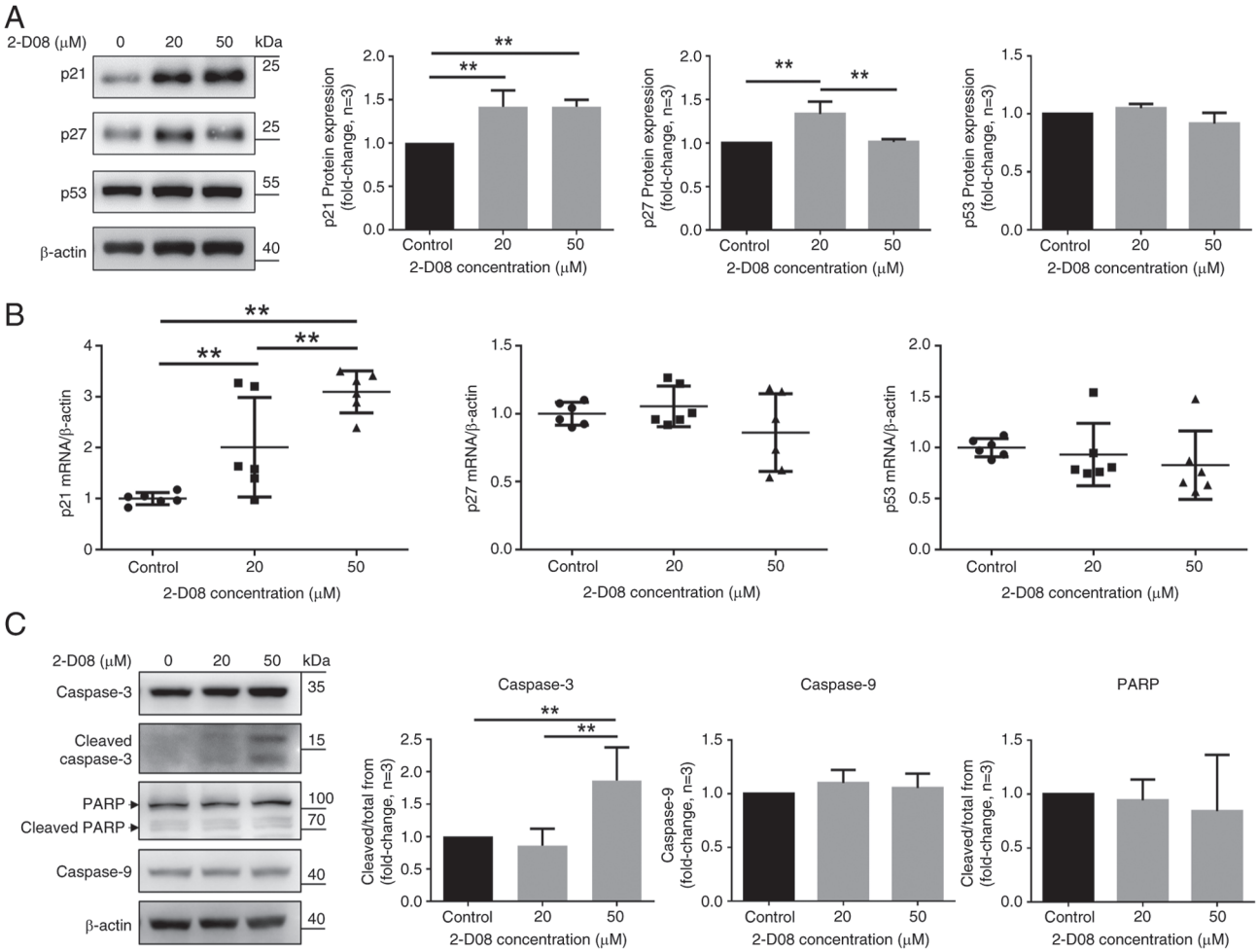

Figure 5. The effects of 2-D08 on the expression of cell proliferation- and apoptosis-associated genes in SK-LMS-1 cells. (A) Expression of p21, p27 and p53 proteins in SK-LMS-1 cells exposed to 2-D08. The bar graph shows the density ratios of the p21, p27 and p53 protein bands relative to β-actin bands. (B) The mRNA levels of p21, p27 and p53 were assessed using reverse transcription-quantitative PCR analysis. The results are presented as the mean ± SEM (n=6). (C) Western blot analysis of the effect of 2-D08 on the activation and proteolytic cleavage by Caspase-3, Caspase-9 and PARP in the SK-LMS-1 cells. The bands in the left panel were quantified using an image analyzer. The data are presented as the mean ± SEM of three independent experiments. **P<0.01 compared with each group. 2-D08, 2',3',4'-trihydroxyflavone; SEM, standard error of the mean.

protein synthesis in SK-LMS-1 and SK-UT-1B cells to evaluate the expression of p53. When treated with CHX for the indicated time, the expression of the p53 protein remained unchanged in SK-LMS-1 cells but decreased in SK-UT-1B cells (Fig. S1). The mRNA levels of p21, but not of p27 and p53, significantly increased compared with the group treated with 2-D08 (Fig. 5B). To improve understanding of how 2-D08 triggers apoptosis in SK-LMS-1 cells, western blot analysis was conducted by investigating the expression of Caspase-3, the pro-apoptotic protein cleaved Caspase-3, Caspase-9 and PARP antibodies with cell lysates. Caspase-3 cleavage was detected under these conditions, indicating that 2-D08 activated Caspase-3 at a concentration of 50 μM (Fig. 5C). By contrast, there was no change in the expression of Caspase-9 or PARP (Fig. 5C). Together, these findings suggested that the modulation of cell cycle- and apoptosis-related proteins may contribute to the 2-D08-induced suppression of proliferation and apoptosis in SK-LMS-1 cells.

Effect of 2-D08 on the expression of differentiation marker proteins in SK-LMS-1 cells. The contractile apparatus of SMCs is characterized by the presence of high levels of α-SM-actin, calponin 1, TAGLN (SM22α) and SM-MHC, which are specific markers of the stage of cell differentiation (34,35). Various SMC malignancies can modulate the differentiated-to-differentiated phenotype in response to changes in the surrounding environment (36-40). For example, the expression of SM-specific markers in human Ut-LMS cell lines, including SK-LMS-1, is low because these cancerous cells have a dedifferentiated SMC phenotype (40). It was investigated whether 2-D08 affects the expression of SM-specific markers. As demonstrated in Fig. 6A, compared with the control group, treatment of SK-LMS-1 cells with 2-D08 did not significantly affect the expression of α-SM-actin, TAGLN, or calponin 1. Furthermore, the mRNA levels of SM-specific markers, excluding TAGLN, did not change significantly compared with those in the group treated with 2-D08 (Fig. 6B). Taken together, these findings demonstrated that 2-D08 does not directly regulate the phenotypic modulation of SK-LMS-1 cells.

Transcriptome analysis in 2-D08-treated SK-LMS-1 cells. It was aimed to obtain additional insights into the effects of

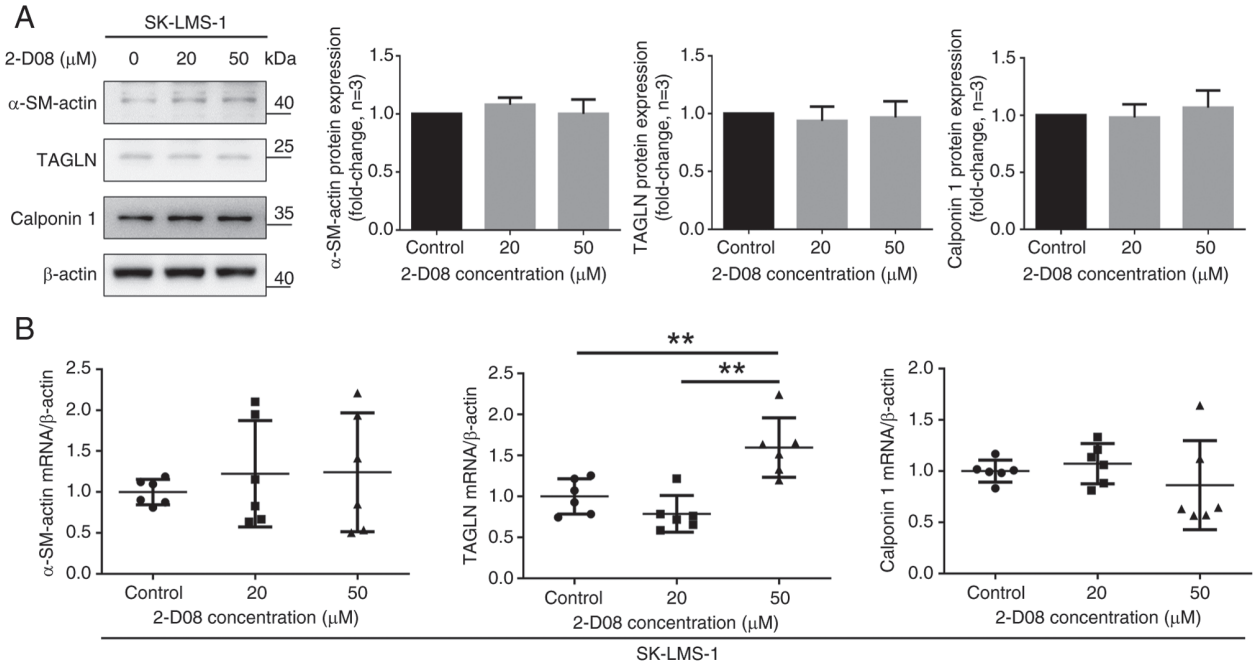

Figure 6. Expression of contractile SMC-specific proteins analyzed using western blot analysis and RT-qPCR in SK-LMS-1 cells treated with 2-D08. (A) The expression of α-SM-actin, TAGLN, and Calponin 1 were assessed using western blot analysis. The bands in the left panel were quantified using an image analyzer. The results are represented as the mean ± SEM (n=3). (B) The mRNA levels of α-SM-actin, TAGLN and Calponin 1 were assessed using RT-qPCR. The results are presented as the mean ± SEM (n=6). **P<0.01. 2-D08, 2',3',4'-trihydroxyflavone; RT-qPCR, reverse transcription-quantitative PCR; SEM, standard error of the mean.

2-D08 and conducted transcriptome analyses with RNA-seq in both control and SK-LMS-1 cells treated with 50 μM 2-D08 for 48 h. Principal component analysis revealed clear clustering per treatment, indicating significant differences in the transcriptome profiles between the two groups (Fig. 7A). The hierarchical clustering heatmap showed that 259 genes were differentially expressed between these two groups (Fig. 7B, adjusted P-value <1.3 and |log2 fold change (FC)|>2). Of the 259 genes, the expression of 192 was upregulated and that of 67 was downregulated in 2-D08-treated SK-LMS-1 cells. The genes with high FCs are listed in Table I and all genes with significantly altered expression are included in Table SII. To obtain information on 2-D08-specific target genes in SK-LMS-1 cells, DEseq2 was utilized to identify differentially expressed genes (DEGs). This analysis revealed that the expression of 1,031 genes was downregulated and that of 2,907 genes was upregulated in 2-D08-treated SK-LMS-1 cells compared with those in the control (adjusted P-value <0.05 and |log2FC|>1). The distribution of DEGs is illustrated in a volcano plot (Fig. 7C). DEGs between the two groups were also examined using edgeR. As revealed in Fig. S2, 3,827 DEGs were identified, with 2,834 showing upregulated expression and 993 showing downregulated expression in two groups. Using gene ontology (GO) functional analysis, statistically significant enrichment was identified for numerous GO biological processes related to DNA replication (cell cycle) between the two groups (Fig. 7D). Gene set enrichment analysis observed that DNA replication (normalized enrichment score=2.35) and DNA-dependent DNA replication (normalized enrichment score=2.509) were positively regulated in the 2-D08-treated group (Fig. 7E). Additionally, various GO molecular functions related to the apoptotic process were significantly enriched (Fig. 7F). Taken together, these findings suggested that 2-D08 modulates pathways related to the cell cycle and apoptosis in SK-LMS-1 cells.

Discussion

In the present study, a new function of 2-D08 in inducing multiple signaling pathways in Ut-LMS cells was identified, including ROS generation, which serve as key mediators of its anticancer effects (Fig. 8). Although 2-D08 is currently known as a SUMO inhibitor, several studies have shown that it participates in numerous biological functions in different cells (22-24). Recently, 2-D08 was shown to suppress the proliferation and differentiation of C2C12 myoblast cells (25). In the current study, the hypothesis that 2-D08 can affect the proliferation of Ut-LMS *in vitro* was tested. The data revealed that 2-D08 suppressed cell viability and enhanced anticancer effects in Ut-LMS cells (Fig. 1B and C). In particular, both low-dose (10-20 μM) and high-dose (50-100 μM) treatment with 2-D08 significantly inhibited long-term colony formation compared with that in the control (Fig. 1E). Furthermore, the data revealed that inhibition of proliferation mediated by 2-D08 was accompanied by induction in the rate of apoptosis in Ut-LMS cells (Figs. 2A and 3B). Interestingly, after 48 h of treatment with 20 μM 2-D08, there was a significant decrease in Ki67 expression (Fig. 4A), indicating reduced cell proliferative activity. However, there was no change in cell viability as measured by the MTT assay (Fig. 1B), suggesting that this decrease in Ki67 expression did not affect the survival ability of the cells. ROS induces lipid peroxidation, which is used as a cell death signal to induce programmed cell death (41). According to a previous study,

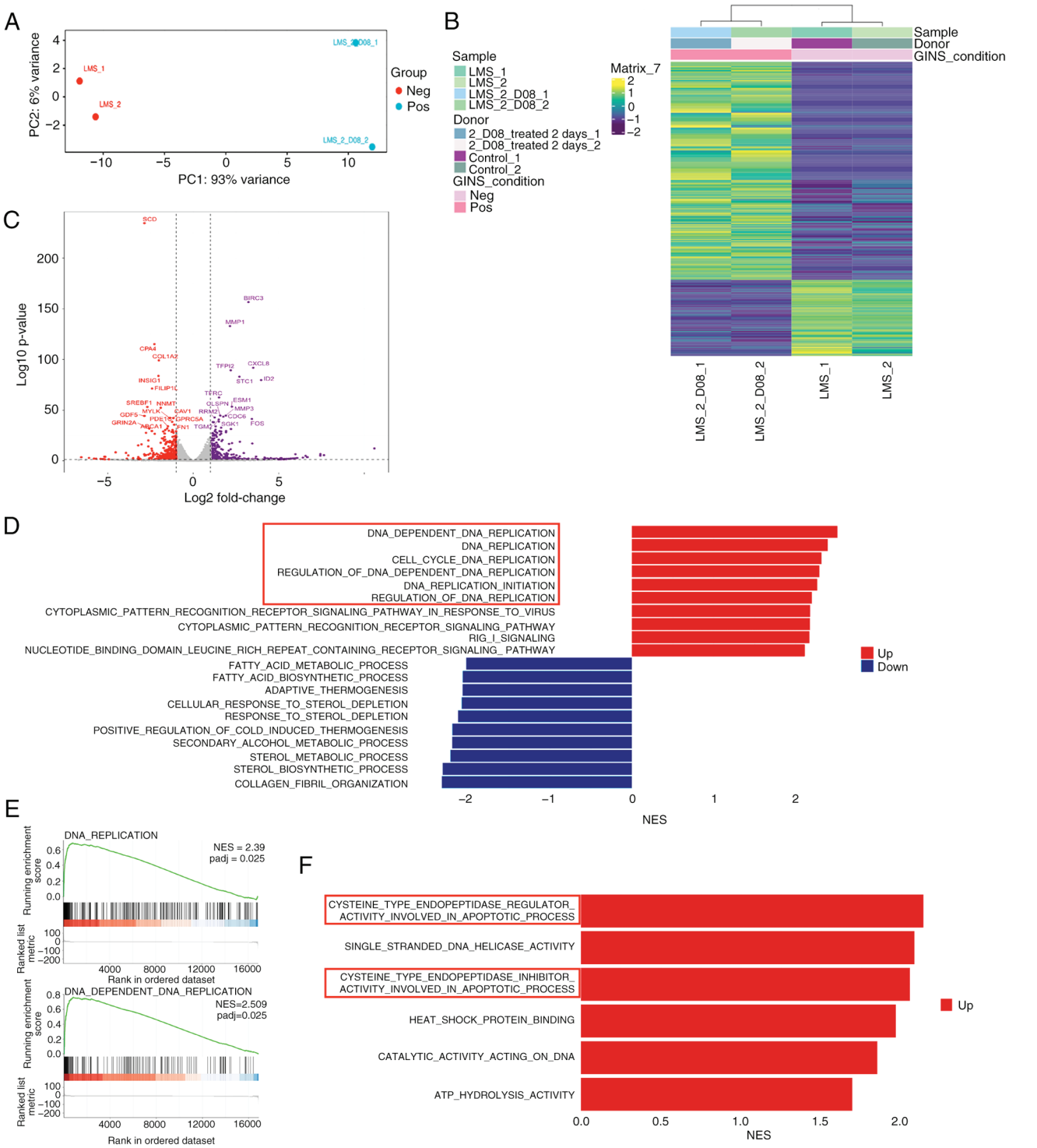

Figure 7. Transcriptome analysis of RNA-sequencing data for 2-D08-treated SK-LMS-1 cells. (A) Principal component analysis plot displaying two groups along PC1 and PC2, which describe 93 and 6% of the variance, respectively. (B) Differential gene expression is shown in the heatmap. Each line with two biological replicates. DEGs were defined by absolute log2 fold change (FC) >2 and P-value <1.3. Blue and yellow indicate low and high gene expression levels, respectively. (C) Volcano plot showing DEGs in control vs. 2-D08-treated cells. Differences in expression are considered significant for |log2FC|>1 and P-value <0.05. Genes with downregulated and upregulated expression are indicated in red and violet, respectively. Dark grey dots indicate non-significant differential gene expression. (D and E) GO analysis revealed the major biological processes and gene set enrichment analysis of the regulated pathways in the control vs. 2-D08-treated cells. (F) GO analysis revealed the molecular functions enriched in the control vs. 2-D08-treated cells. 2-D08, 2',3',4'-trihydroxyflavone; DEGs, differentially expressed genes; GO, Gene Ontology.

2-D08 induces ROS accumulation and mediates apoptosis in acute myeloid leukemia cells (24). Consistent with the results of previous studies (24), the results of the present study revealed that induction of apoptosis by 2-D08 was significantly influenced by ROS accumulation in SK-LMS-1 cells (Fig. 3A). Furthermore, these results indicated the presence of basal ROS levels in SK-LMS-1 cells and supported the notion that cancer cells exhibit higher basal levels of ROS compared

Table I. High fold-change genes among the significantly up- and downregulated genes.

Gene symbol	Description	log2FoldChange	P-value
Upregulated genes top 10-fold change			
HSPA6	Heat shock protein family A (Hsp70) member 6	10.56313299	12.14147123
TINCR	TINCR ubiquitin domain containing	7.622131682	5.477771463
RASD1	Ras related dexamethasone induced 1	7.409021026	6.643901651
FRG2B	FSHD region gene 2 family member B	7.403884047	5.03755407
RIMBP3C	RIMS binding protein 3C	6.660468995	3.55968452
AFF2	ALF transcription elongation factor 2	6.633655223	3.527869717
ARC	Activity regulated cytoskeleton associated protein	6.546234801	4.829959694
ASXL3	ASXL transcriptional regulator 3	6.386994619	3.064184081
FCRL3	Fc receptor like 3	6.070912873	2.678081617
CCDC73	Coiled-coil domain containing 73	6.057297181	2.670620262
Downregulated genes top 10-fold change			
LCN12	Lipocalin 12	-4.939386897	1.359228814
CCN5	Cellular communication network factor 5	-5.149869976	3.976541161
TNFSF12-TNFSF13	TNFSF12-TNFSF13 readthrough	-5.177935809	1.336744493
ABCG1	ATP binding cassette subfamily G member 1	-5.202302215	4.051255441
MUSTN1	Musculoskeletal, embryonic nuclear protein 1	-5.277064096	1.669719597
tspan32	tetraspanin 32	-5.420116874	1.814259284
CPAMD8	C3 and PZP like alpha-2-macroglobulin domain containing 8	-5.683960725	2.050450132
TBC1D3C	TBC1 domain family member 3C	-5.804635788	2.100940952
URGCP-MRPS24	URGCP-MRPS24 readthrough	-6.100406013	2.762892929
ATF7-NPFF	ATF7-NPFF readthrough	-6.546939056	3.447437941

with normal cells due to an imbalance between oxidants and antioxidants (42).

According to previous studies, p21, p27 and p53 are direct or indirect suppressors of tumor development and play different roles in human biological systems (43). Uterine leiomyosarcomas are characterized by increased p53 expression compared with normal leiomyomas and SM tumors of uncertain malignant potential (44,45). Additionally, upregulation of p21 expression contributes to cell cycle arrest by activating p53 (46). Consistent with these studies, it was hypothesized that 2-D08 affects the expression of p21, p27 and p53 in SK-LMS-1 cells. The antiproliferative effects of low-dose (20 μM) 2-D08 treatment for 48 h and the significant increase in the expression levels of p21 and p27 proteins were demonstrated in Fig. 5A. The expression of p21 protein only increased when 2-D08 was supplied at a high dose (50 μM) through the induction of antiproliferative activity and arrest at the S and G2/M phases (Fig. 4D, bottom panels). This is an important strategy in cancer treatment, as it inhibits the proliferation and division of cancer cells by interfering with the cell cycle that regulates cell division. Therefore, these results indicated that p21 and p27 can act individually under each experimental condition and that p21 is more strongly associated with the 2-D08-induced effects against cell proliferation than p27. However, as shown in Fig. 1E, p27 may also be involved in the inhibition of Ut-LMS cell proliferation at low doses of long-term 2-D08 treatment. Interestingly, the protein level of p53 was not significantly related to either dose (Fig. 5A), and 2-D08 triggered apoptosis in these cells possibly through enhanced expression of cleaved Caspase-3 at a high dose (50 μM) (Figs. 3B and 5C). Additional experiments are required to verify these differences and further confirm the mechanism involved.

Unlike cardiac or skeletal muscle cells, SMCs are unique in their capacity to switch phenotypes (39,47,48). SMC phenotypic conversion has been extensively investigated in vascular diseases such as atherosclerosis (49). Although vascular SMC conversion has been intensively studied, phenotypic modulation appears to strongly correlate with the development of Ut-LMS. In a study published in 2010, a less-differentiated SMC phenotype was observed in human Ut-LMS cell lines, whereas the exogenous expression of myocardin in Ut-LMS cells induced increased expression of SM-specific markers and stabilization of actin fibers (40). Thus, despite the assumption that 2-D08 is associated with an altered phenotype of SK-LMS-1 cells, the expression of SMC marker genes did not change significantly in 2-D08-treated-SK-LMS-1 cells (Fig. 6A). These results suggested that 2-D08 represents an antiproliferative and apoptotic effector rather than a phenotypic modulator in SK-LMS-1 cells. Although the mechanisms

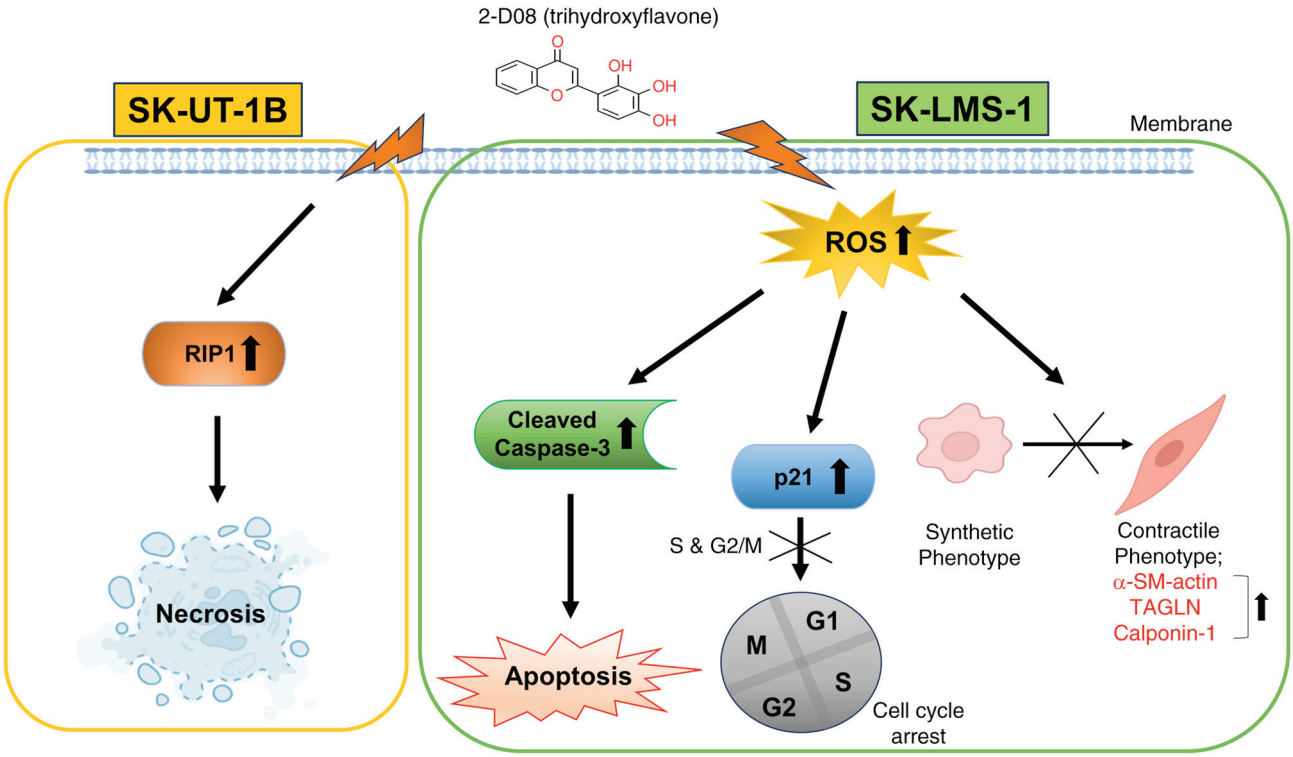

Figure 8. 2-D08 modulates multiple cellular pathways to exert its antitumor effect in uterine leiomyosarcoma cells. 2-D08, 2',3',4'-trihydroxyflavone.

underlying 2-D08-mediated phenotypic conversion remain unclear, other candidate genes or drugs may play pivotal roles in the phenotypic conversion of Ut-LMS.

Transcriptome analysis of 2-D08-treated SK-LMS-1 cells revealed significant changes in gene expression, with 259 genes differentially expressed and distinct clustering observed for each treatment group (Fig. 7B). The analysis identified 2-D08-specific target genes and showed downregulated expression for 1,031 genes and upregulated expression for 2,907 genes in 2-D08-treated cells (Fig. 7C; Table SII). GO functional analysis revealed significant enrichment for biological processes related to DNA replication (cell cycle) and various molecular functions related to the apoptotic process (Fig 7D-F). These findings suggested that 2-D08 modulates pathways related to the cell cycle and apoptosis in SK-LMS-1 cells, and potentially offers a new therapeutic strategy against cancer. The exact molecular mechanisms through which 2-D08 modulates the cell cycle and apoptotic pathways in SK-LMS-1 cells are not fully understood and require further research. It is also important to note that, while this analysis provides valuable insights into the potential effects of 2-D08 on Ut-LMS cells, additional studies are needed to validate these findings and explore their broader implications.

Analysis of RNA-seq data has revealed that treatment with 2-D08 enhances the expression of dexamethasone-induced Ras-related protein 1 (RASD1), a key estrogen signal transducer in female reproductive organs (50,51). Rapid upregulation of the expression of RASD1 induced by estrogen occurs via the p38-MAPK and ERK1/2 pathways in ovariectomized and prepubertal mice. Reduced expression of RASD1 in patients with repeated implantation failure correlates with lower estrogen levels during the menstrual cycle, suggesting impaired implantation (50). Under normal conditions, RASD1 facilitates uterine modulation for successful implantation, while decreased levels in patients with repeated implantation failure result in abnormal uterine regulation, hindering implantation (51). Additionally, RASD1 overexpression suppresses cell proliferation in various cell types, including NIH-3T3 fibroblast cells, MCF-7 breast cancer, and A549 lung adenocarcinoma cell lines (52). Further studies are needed to improve understanding of the relationship between 2-D08 and RASD1 and to gain clinical insights into uterine leiomyosarcoma.

A significant decrease in viability and colony formation capacity was observed in SK-UT-1B cells, demonstrating an anticancer effect (Fig. 1C and E). However, the experiments related to the cell cycle using flow cytometry did not demonstrate any effect of 2-D08 on SK-UT-1B cells compared with the results with SK-LMS-1 cells (Fig. 2B). Even though SK-LMS-1 and SK-UT-1B are both LMS cell lines, differences in gene expression due to cell origin appear to have led to these results. As depicted in Fig. S1, a CHX assay was conducted to inhibit protein synthesis and no difference was observed in the expression of p53 in SK-LMS-1 cells, although, a decrease was observed in SK-UT-1B cells, in the indicated timepoints. These results suggested that the stability of p53 may differ between the two cell lines. The difference in p53 protein stability between the two cell lines is likely attributed to variations in mutation sites within the p53 gene (53,54), but further research is needed for confirmation. Additionally, SK-UT-1B is slightly faster in doubling time compared with SK-LMS-1, as indicated by a previous study (55). Despite conducting a comprehensive cell cycle analysis, no clear relationship was found between the doubling times of cell lines with similar histology or those with similar doubling times. Furthermore, 2-D08 is involved

in various signaling pathways such as ROS, apoptosis and proliferation in SK-LMS-1 cells compared with SK-UT-1B cells. Studying the changes in gene expression related to these signaling pathways could lead to the development of substances targeting them, maximizing their anticancer effects. To investigate which genes are involved in these signaling pathways and contribute to the anticancer effect of 2-D08, RNA-seq analysis was performed on SK-LMS-1 cells treated with 2-D08 (Fig. 7). Therefore, further studies on the mechanism in Ut-LMS cell lines can help to more clearly define the direction of LMS treatment, considering that the response to cancer therapy can vary greatly depending on individual genetic differences. Such research contributes to the personalization of cancer management and plays an important role in determining the most effective treatment for specific patient groups.

Among the limitations of this study, the authors acknowledge that extensive research using, for example, animal models is warranted to determine the biological effects of 2-D08 and the mechanisms underlying its roles. In addition, most *in vitro* experiments were conducted using two short-term (48 h) doses (20 and 50 μM) of 2-D08. Selection of the optimal dose of 2-D08 is required for treating human Ut-LMS. Lastly, using established Ut-LMS treatment drugs such as trabectedin, pazopanib and dacarbazine as positive controls in the present study could enhance reliability. However, it remains unclear which signaling pathways mediate the effects of these drugs in Ut-LMS cell lines.

In summary, the present study demonstrated that 2-D08 elicits anticancer effects via multiple signaling pathways in Ut-LMS cells. Although additional research is needed to fully understand the underlying biological mechanisms, these results suggested that treatment with 2-D08 can repress proliferation, induce apoptosis and potentially affect tumor development in Ut-LMS.

Acknowledgements

Not applicable.

Funding

The present study was supported by the Chosun University (grant no. K208554001), the National Research Foundation of Korea (NRF) funded by the Korea government (MSIT) (grant no. NRF-2020R1C1C1003272), the Basic Science Research Program through NRF funded by the Ministry of Education (grant no. NRF-2022R1I1A1A01053069) and the NRF funded by the Korea government (MSIT) (grant no. RS-2022-00166501).

Availability of data and materials

The datasets used and analyzed during the current study are available from the GEO database (accession no. GSE264332).

Authors' contributions

HJ designed the experiments and commented on the manuscript. HL and HJ conducted the experiments and wrote the manuscript. HL and HJ participated in the data analyses and confirm the authenticity of all the raw data. Both authors read and approved the final version of the manuscript.

Ethics approval and consent to participate

Not applicable.

Patient consent for publication

Not applicable.

Competing interests

The authors declare that they have no competing interests.

References

1. Echt G, Jepson J, Steel J, Langholz B, Luxton G, Hernandez W, Astrahan M and Petrovich Z: Treatment of uterine sarcomas. Cancer 66: 35-39, 1990.
2. Kim WY, Chang SJ, Chang KH, Yoon JH, Kim JH, Kim BG, Bae DS and Ryu HS: Uterine leiomyosarcoma: 14-year two-center experience of 31 cases. Cancer Res Treat 41: 24-28, 2009.
3. Tirumani SH, Deaver P, Shinagare AB, Tirumani H, Hornick JL, George S and Ramaiya NH: Metastatic pattern of uterine leiomyosarcoma: Retrospective analysis of the predictors and outcome in 113 patients. J Gynecol Oncol 25: 306-312, 2014.
4. Chern JY, Boyd LR and Blank SV: Uterine sarcomas: The latest approaches for these rare but potentially deadly tumors. Oncology (Williston Park) 31: 229-236, 2017.
5. Murakami M, Ichimura T, Kasai M, Matsuda M, Kawamura N, Fukuda T and Sumi T: Examination of the use of needle biopsy to perform laparoscopic surgery safely on uterine smooth muscle tumors. Oncol Lett 15: 8647-8651, 2018.
6. Hernando E, Charytonowicz E, Dudas ME, Menendez S, Matushansky I, Mills J, Socci ND, Behrendt N, Ma L, Maki RG, *et al*: The AKT-mTOR pathway plays a critical role in the development of leiomyosarcomas. Nat Med 13: 748-753, 2007.
7. Babichev Y, Kabaroff L, Datti A, Uehling D, Isaac M, Al-Awar R, Prakesch M, Sun RX, Boutros PC, Venier R, *et al*: PI3K/AKT/mTOR inhibition in combination with doxorubicin is an effective therapy for leiomyosarcoma. J Transl Med 14: 67, 2016.
8. Gaumann AK, Drexler HC, Lang SA, Stoeltzing O, Diermeier-Daucher S, Buchdunger E, Wood J, Bold G and Breier G: The inhibition of tyrosine kinase receptor signalling in leiomyosarcoma cells using the small molecule kinase inhibitor PTK787/ZK222584 (Vatalanib®). Int J Oncol 45: 2267-2277, 2014.
9. Hayashi T, Horiuchi A, Sano K, Hiraoka N, Kanai Y, Shiozawa T, Tonegawa S and Konishi I: Molecular approach to uterine leiomyosarcoma: LMP2-deficient mice as an animal model of spontaneous uterine leiomyosarcoma. Sarcoma 2011: 476498, 2011.
10. Cancer Genome Atlas Research Network. Electronic address: elizabeth.demicco@sinaihealthsystem.ca and Cancer Genome Atlas Research Network: Comprehensive and integrated genomic characterization of adult soft tissue sarcomas. Cell 171: 950-965. e28, 2017.
11. Mäkinen N, Aavikko M, Heikkinen T, Taipale M, Taipale J, Koivisto-Korander R, Bützow R and Vahteristo P: Exome sequencing of uterine leiomyosarcomas identifies frequent mutations in TP53, ATRX, and MED12. PLoS Genet 12: e1005850, 2016.
12. Tsuyoshi H and Yoshida Y: Molecular biomarkers for uterine leiomyosarcoma and endometrial stromal sarcoma. Cancer Sci 109: 1743-1752, 2018.
13. Hanahan D and Weinberg RA: Hallmarks of cancer: The next generation. Cell 144: 646-674, 2011.
14. DeCensi A, Guerrieri-Gonzaga A, Gandini S, Serrano D, Cazzaniga M, Mora S, Johansson H, Lien EA, Pruneri G, Viale G and Bonanni B: Prognostic significance of Ki-67 labeling index after short-term presurgical tamoxifen in women with ER-positive breast cancer. Ann Oncol 22: 582-587, 2011.

15. Davey MG, Hynes SO, Kerin MJ, Miller N and Lowery AJ: Ki-67 as a prognostic biomarker in invasive breast cancer. Cancers (Basel) 13: 4455, 2021.
16. Tollefson MK, Karnes RJ, Kwon ED, Lohse CM, Rangel LJ, Mynderse LA, Cheville JC and Sebo TJ: Prostate cancer Ki-67 (MIB-1) expression, perineural invasion, and gleason score as biopsy-based predictors of prostate cancer mortality: The mayo model. Mayo Clin Proc 89: 308-318, 2014.
17. Maia R, Santos GAD, Reis S, Viana NI, Pimenta R, Guimarães VR, Recuero S, Romão P, Leite KRM, Srougi M and Passerotti CC: Can we use Ki67 expression to predict prostate cancer aggressiveness? Rev Col Bras Cir 49: e20223200, 2022. (In English, Portuguese)
18. Zhang F, Zhang F, Liu Z, Wu K, Zhu Y and Lu Y: Prognostic role of Ki-67 in adrenocortical carcinoma after primary resection: A retrospective mono-institutional study. Adv Ther 36: 2756-2768, 2019.
19. Akhan SE, Yavuz E, Tecer A, Iyibozkurt CA, Topuz S, Tuzlali S, Bengisu E and Berkman S: The expression of Ki-67, p53, estrogen and progesterone receptors affecting survival in uterine leiomyosarcomas. A clinicopathologic study. Gynecol Oncol 99: 36-42, 2005.
20. Travaglino A, Raffone A, Catena U, De Luca M, Toscano P, Del Prete E, Vecchione ML, Lionetti R, Zullo F and Insabato L: Ki67 as a prognostic marker in uterine leiomyosarcoma: A quantitative systematic review. Eur J Obstet Gynecol Reprod Biol 266: 119-124, 2021.
21. Kim YS, Keyser SG and Schneekloth JS Jr: Synthesis of 2',3',4'-trihydroxyflavone (2-D08), an inhibitor of protein sumoylation. Bioorg Med Chem Lett 24: 1094-1097, 2014.
22. Marsh DT, Das S, Ridell J and Smid SD: Structure-activity relationships for flavone interactions with amyloid beta reveal a novel anti-aggregatory and neuroprotective effect of 2',3',4'-trihydroxyflavone (2-D08). Bioorg Med Chem 25: 3827-3834, 2017.
23. Choi BH, Philips MR, Chen Y, Lu L and Dai W: K-Ras Lys-42 is crucial for its signaling, cell migration, and invasion. J Biol Chem 293: 17574-17581, 2018.
24. Zhou P, Chen X, Li M, Tan J, Zhang Y, Yuan W, Zhou J and Wang G: 2-D08 as a SUMOylation inhibitor induced ROS accumulation mediates apoptosis of acute myeloid leukemia cells possibly through the deSUMOylation of NOX2. Biochem Biophys Res Commun 513: 1063-1069, 2019.
25. Liu H, Lee SM and Joung H: 2-D08 treatment regulates C2C12 myoblast proliferation and differentiation via the Erk1/2 and proteasome signaling pathways. J Muscle Res Cell Motil 42: 193-202, 2021.
26. Livak KJ and Schmittgen TD: Analysis of relative gene expression data using real-time quantitative PCR and the 2(-Delta Delta C(T)) method. Methods 25: 402-408, 2001.
27. Dobin A, Davis CA, Schlesinger F, Drenkow J, Zaleski C, Jha S, Batut P, Chaisson M and Gingeras TR: STAR: Ultrafast universal RNA-seq aligner. Bioinformatics 29: 15-21, 2013.
28. Li B and Dewey CN: RSEM: Accurate transcript quantification from RNA-Seq data with or without a reference genome. BMC Bioinformatics 12: 323, 2011.
29. Love MI, Huber W and Anders S: Moderated estimation of fold change and dispersion for RNA-seq data with DESeq2. Genome Biol 15: 550, 2014.
30. Robinson MD, McCarthy DJ and Smyth GK: edgeR: A bioconductor package for differential expression analysis of digital gene expression data. Bioinformatics 26: 139-140, 2010.
31. Guo C, Sun L, Chen X and Zhang D: Oxidative stress, mitochondrial damage and neurodegenerative diseases. Neural Regen Res 8: 2003-2014, 2013.
32. Nishikawa M, Hashida M and Takakura Y: Catalase delivery for inhibiting ROS-mediated tissue injury and tumor metastasis. Adv Drug Deliv Rev 61: 319-326, 2009.
33. Zhitkovich A: *N*-Acetylcysteine: Antioxidant, aldehyde scavenger, and more. Chem Res Toxicol 32: 1318-1319, 2019.
34. Beamish JA, He P, Kottke-Marchant K and Marchant RE: Molecular regulation of contractile smooth muscle cell phenotype: Implications for vascular tissue engineering. Tissue Eng Part B Rev 16: 467-491, 2010.
35. Xie C, Ritchie RP, Huang H, Zhang J and Chen YE: Smooth muscle cell differentiation in vitro: Models and underlying molecular mechanisms. Arterioscler Thromb Vasc Biol 31: 1485-1494, 2011.
36. Amada S, Nakano H and Tsuneyoshi M: Leiomyosarcoma versus bizarre and cellular leiomyomas of the uterus: A comparative study based on the MIB-1 and proliferating cell nuclear antigen indices, p53 expression, DNA flow cytometry, and muscle specific actins. Int J Gynecol Pathol 14: 134-142, 1995.
37. Sprogøe-Jakobsen S and Hølund B: Immunohistochemistry (Ki-67 and p53) as a tool in determining malignancy in smooth muscle neoplasms (exemplified by a myxoid leiomyosarcoma of the uterus). APMIS 104: 705-708, 1996.
38. Horiuchi A, Nikaido T, Ito K, Zhai Y, Orii A, Taniguchi S, Toki T and Fujii S: Reduced expression of calponin h1 in leiomyosarcoma of the uterus. Lab Invest 78: 839-846, 1998.
39. Owens GK, Kumar MS and Wamhoff BR: Molecular regulation of vascular smooth muscle cell differentiation in development and disease. Physiol Rev 84: 767-801, 2004.
40. Kimura Y, Morita T, Hayashi K, Miki T and Sobue K: Myocardin functions as an effective inducer of growth arrest and differentiation in human uterine leiomyosarcoma cells. Cancer Res 70: 501-511, 2010.
41. Wang B, Wang Y, Zhang J, Hu C, Jiang J, Li Y and Peng Z: ROS-induced lipid peroxidation modulates cell death outcome: Mechanisms behind apoptosis, autophagy, and ferroptosis. Arch Toxicol 97: 1439-1451, 2023.
42. Nakamura H and Takada K: Reactive oxygen species in cancer: Current findings and future directions. Cancer Sci 112: 3945-3952, 2021.
43. Philipp-Staheli J, Kim KH, Liggitt D, Gurley KE, Longton G and Kemp CJ: Distinct roles for p53, p27Kip1, and p21Cip1 during tumor development. Oncogene 23: 905-913, 2004.
44. O'Neill CJ, McBride HA, Connolly LE and McCluggage WG: Uterine leiomyosarcomas are characterized by high p16, p53 and MIB1 expression in comparison with usual leiomyomas, leiomyoma variants and smooth muscle tumours of uncertain malignant potential. Histopathology 50: 851-858, 2007.
45. Schaefer IM, Hornick JL, Sholl LM, Quade BJ, Nucci MR and Parra-Herran C: Abnormal p53 and p16 staining patterns distinguish uterine leiomyosarcoma from inflammatory myofibroblastic tumour. Histopathology 70: 1138-1146, 2017.
46. Bunz F, Dutriaux A, Lengauer C, Waldman T, Zhou S, Brown JP, Sedivy JM, Kinzler KW and Vogelstein B: Requirement for p53 and p21 to sustain G2 arrest after DNA damage. Science 282: 1497-1501, 1998.
47. Le Guen L, Marchal S, Faure S and de Santa Barbara P: Mesenchymal-epithelial interactions during digestive tract development and epithelial stem cell regeneration. Cell Mol Life Sci 72: 3883-3896, 2015.
48. Scirocco A, Matarrese P, Carabotti M, Ascione B, Malorni W and Severi C: Cellular and molecular mechanisms of phenotypic switch in gastrointestinal smooth muscle. J Cell Physiol 231: 295-302, 2016.
49. Chakraborty R, Chatterjee P, Dave JM, Ostriker AC, Greif DM, Rzucidlo EM and Martin KA: Targeting smooth muscle cell phenotypic switching in vascular disease. JVS Vasc Sci 2: 79-94, 2021.
50. Kim HR, Cho KS, Kim E, Lee OH, Yoon H, Lee S, Moon S, Park M, Hong K, Na Y, *et al*: Rapid expression of RASD1 is regulated by estrogen receptor-dependent intracellular signaling pathway in the mouse uterus. Mol Cell Endocrinol 446: 32-39, 2017.
51. Hong K and Choi Y: Role of estrogen and RAS signaling in repeated implantation failure. BMB Rep 51: 225-229, 2018.
52. Vaidyanathan G, Cismowski MJ, Wang G, Vincent TS, Brown KD and Lanier SM: The Ras-related protein AGS1/RASD1 suppresses cell growth. Oncogene 23: 5858-5863, 2004.
53. Park DJ, Nakamura H, Chumakov AM, Said JW, Miller CW, Chen DL and Koeffler HP: Transactivational and DNA binding abilities of endogenous p53 in p53 mutant cell lines. Oncogene 9: 1899-1906, 1994.
54. Smardová J, Pavlová S, Svitáková M, Grochová D and Ravcuková B: Analysis of p53 status in human cell lines using a functional assay in yeast: detection of new non-sense p53 mutation in codon 124. Oncol Rep 14: 901-907, 2005.
55. Mills J, Matos T, Charytonowicz E, Hricik T, Castillo-Martin M, Remotti F, Lee FY and Matushansky I: Characterization and comparison of the properties of sarcoma cell lines in vitro and in vivo. Hum Cell 22: 85-93, 2009.